

Article

A Senescence-Like Cellular Response Inhibits Bovine Ephemeral Fever Virus Proliferation

Yu-Jing Zeng¹, Min-Kung Hsu², Chiao-An Tsai³, Chun-Yen Chu^{1,3}, Hsing-Chieh Wu¹ and Hsian-Yu Wang^{1,3,*}

¹ International Program in Animal Vaccine Technology, International College, National Pingtung University of Science and Technology, Pingtung 91201, Taiwan; J10885002@mail.npust.edu.tw (Y.-J.Z.); cychu@mail.npust.edu.tw (C.-Y.C.); hcwu@mail.npust.edu.tw (H.-C.W.)

² Research Center for Tumor Medical Science, China Medical University, Taichung 40402, Taiwan; mkh@tms.cmu.edu.tw

³ Graduate Institute of Animal Vaccine Technology, College of Veterinary Medicine, National Pingtung University of Science and Technology, Pingtung 91201, Taiwan; ananbirdhome@yahoo.com.tw

* Correspondence: hyw@mail.npust.edu.tw

Abstract: During industrial-scale production of viruses for vaccine manufacturing, anti-viral response of host cells can dampen maximal viral antigen yield. In addition to interferon responses, many other cellular responses, such as the AMPK signaling pathway or senescence-like response may inhibit or slow down virus amplification in the cell culture system. In this study, we first performed a Gene Set Enrichment Analysis of the whole-genome mRNA transcriptome and found a senescence-like cellular response in BHK-21 cells when infected with bovine ephemeral fever virus (BEFV). To demonstrate that this senescence-like state may reduce virus growth, BHK-21 subclones showing varying degrees of a senescence-like state were infected with BEFV. The results showed that the BHK-21 subclones showing high senescence staining could inhibit BEFV replication while low senescence-staining subclones are permissive to virus replication. Using a different approach, a senescence-like state was induced in BHK-21 using a small molecule, camptothecin (CPT), and BEFV susceptibility were examined. The results showed that CPT-treated BHK-21 is more resistant to virus infection. Overall, these results indicate that a senescence-like response may be at play in BHK-21 upon virus infection. Furthermore, cell clone selection and modulating treatments using small molecules may be tools in countering anti-viral responses.

Keywords: anti-viral response; senescence-like response; viral vaccine production; BEFV; *Rhabdoviridae*; GSEA; BHK-21; bioreactor



Citation: Zeng, Y.-J.; Hsu, M.-K.; Tsai, C.-A.; Chu, C.-Y.; Wu, H.-C.; Wang, H.-Y. A Senescence-Like Cellular Response Inhibits Bovine Ephemeral Fever Virus Proliferation. *Vaccines* **2021**, *9*, 601. <https://doi.org/10.3390/vaccines9060601>

Academic Editor: Steven B. Bradfute

Received: 6 April 2021

Accepted: 31 May 2021

Published: 4 June 2021

Publisher's Note: MDPI stays neutral with regard to jurisdictional claims in published maps and institutional affiliations.



Copyright: © 2021 by the authors. Licensee MDPI, Basel, Switzerland. This article is an open access article distributed under the terms and conditions of the Creative Commons Attribution (CC BY) license (<https://creativecommons.org/licenses/by/4.0/>).

1. Introduction

Successful virus production using cell cultures depends, in large part, on the response of the host cells. Some cell lines, such as CHO, are highly resistant to virus infection due to their strong anti-viral interferon response. In contrast, some cell lines, such as Vero and BHK-21, exhibit low interferon response and are, therefore, more amenable to virus production for purposes such as vaccine manufacturing [1–3]. Upon virus infection, in addition to interferon responses, a host of other cellular stress responses may also come into play inside the host cell: senescence-like response, the AMP-activated protein kinase (AMPK) signaling pathway, or innate immune responses that can inhibit or slow down virus amplification. These anti-viral responses may be further enhanced in the large-scale bioreactor because of the multiple amplification of the production cells in the culture vessel. Understanding and managing the anti-viral responses of the host cell are critical steps in the development of an optimal virus culturing system.

Bovine ephemeral fever virus (BEFV) belongs to the *Rhabdoviridae* family with a single-stranded, negative sense RNA genome that encodes five structural proteins (N, P, M, G, and L) and a nonstructural proteins [4–7]. Although mortality due to BEFV infection is

low, reduced milk production during pandemic periods can result in significant economic losses for dairy farms [8]. While inactivated BEFV vaccines provide sufficient protection, immunity decreases rapidly and cattle need to be vaccinated every one to two years [9]. Therefore, the stable production of this virus as a vaccine antigen is important for the cattle industry.

BHK-21 is widely used for BEFV production because of its high virus susceptibility. Clear cytopathic effect (CPE) and cell death can be observed 48 hr after BEFV infection. However, some BHK-21 cells appear not to show CPE, remain alive, and can even be passaged. The survival of these cells could mean that the virus production system is less efficient; thus, it is important to explore potential explanations for the survival of some BHK-21 cells after BEFV infection. In previous studies, not only the foot-and-mouth disease virus, but also the rabies virus, reported a persistent infection in BHK-21 cells [10,11]. We also noticed that the BEFV-persistent infected BHK-21 cells gain an enlarged and flattened morphology which is similar to the senescence cells described by the other researchers [12,13].

In this study, we first performed a cell functional analysis of BEFV-infected BHK-21 cells to look for gene sets that become enriched after infection. Enriched gene sets may point to potential pathways of anti-viral response. We then hypothesized that a senescence-like state may play a role in the virus resistance of some BHK-21 cells. As supporting evidence, we performed two experiments: (1) subclones of BHK-21 were stained for senescence-like state and their resistance to BEFV infection was studied, and (2) a senescence-like state, induced in BHK-21 using a small-molecule, camptothecin (CPT), and BEFV susceptibility, was examined.

2. Materials and Methods

2.1. BEFV Culture and Quantification

Baby Hamster Kidney-21 cells (BHK-21, BCRC#60041, purchased from the Bio-resource Collection and Research Center, Hsinchu, Taiwan), were cultured in growth medium (MEM, Gibco Co. Ltd., New York, NY, USA, with 10% FBS, Invitrogen) at 37 °C in an atmosphere of 5% CO₂. The BEFV strain Tn88128 isolated in Taiwan [4] was cultured in BHK-21 cells (MOI = 0.01) in 2% FBS media (MEM media containing 2% FBS) at 37 °C with 5% CO₂. The mock group cells were incubated with the 2% FBS media only. Virus titer was determined by the TCID₅₀ or q-RTPCR method. For TCID₅₀, CPE was observed under the microscope 3 days after inoculation and calculated by using the Reed and Muench method [14]. For q-PCR analysis of virus titer, viral RNA was isolated with QIAzol Lysis Reagent (Qiagen Co. Ltd., Crawley, WV, USA). After reverse-transcription by the SensiFAST™ cDNA Synthesis Kit (Bioline, Memphis, TN, USA), cDNA samples were prepared with the QuantiFast SYBR Green PCR Master Mix reagent (Qiagen, Hilden, Germany) with the detection primers (BEFV-G F: 5'-TACCCTCCTGCTGGATGCTTTTG-3' and BEFV-G R: 5'-CTGTGTGCATTCTAAAACCTGGC-3'). Real-time PCR conditions were 95 °C for 3 min, followed by 40 cycles at 95 °C for 15 s, 60 °C for 30 s and 72 °C for 15 s. The virus titer was determined by comparison to the standard virus stock, and shown as TCID₅₀/mL.

2.2. Cell Functional Analysis for Surviving BHK-21 Cells after BEFV Infection (Gene Set Enrichment Analysis, GSEA)

BHK-21 cells were inoculated with BEFV and total cellular mRNA were harvested at the indicated time with the QIAzol Lysis Reagent (Qiagen Co. Ltd., Crawley, WV, USA) according to the protocol of the manufacturer. Total cDNA was prepared by the SensiFAST™ cDNA Synthesis Kit (Bioline, Memphis, TN, USA) and analyzed by next generation sequencing service (Illumina, 150 pb pair end, 6G, Tools Co. Ltd. Taipei, Taiwan). All NGS samples were aligned to the BHK-21 genome (*Mesocricetus_auratus*. MesAur 1.0.98) by using the STAR aligner [15,16]. The gene expressions were determined as FPKM by using the Cufflinks [17] to assemble and quantify FPKM transcripts. To evaluate the biological pathways altered between BEFV-infected BHK-21 cell and mock-infected

BHK-21, the Gene Set Enrichment Analysis (GSEA) (Broad Institute, Cambridge, MA, USA, java GSEA Desktop Application version 4.1.0) [18,19] tool was employed. The KEGG pathway gene subsets of GSEA Molecular Signatures Database (MSigDB) [18] C2-curated gene sets (186 gene sets), along with external senescence-related gene subsets, were applied to enrichment analysis (total 204 gene sets). The external senescence-related gene subsets were added in the analysis, as the references described in Supplementary Table S1. Gene set enrichment was considered significant at $FDR < 0.25$ [18].

2.3. BHK-21 Subclones Isolation

To isolate subclones of BHK-21, parental BHK-21 cells were trypsinized and resuspended in growth media for calculation. The resuspended cells were diluted into 1 cell/0.1 mL density and seeded into 96-well plates (Corning, Co. Ltd., Kennebunk, ME, USA) (0.1 mL/well). Confluent cells were then subcultured into 24-well and 6-well plates (Corning, Co. Ltd., Kennebunk, ME, USA) sequentially. Subclones were then stored in freezing media (growth media with 7% DMSO) at $-80\text{ }^{\circ}\text{C}$ for further use.

2.4. Senescence-Like-Associated SA- β -Galactosidase Staining

SA- β -gal staining was chosen as the senescence marker [20] and performed according to a protocol published by Dimri et al., 1995 [21]. Cells were washed twice with PBS and fixed by 4% paraformaldehyde for 5 min at room temperature. The fixed cells were stained with the SA- β -Gal staining solution (1 mg/mL X-Gal in dimethylformamide, pH 6.0 citric acid/sodium phosphate buffer, 5 mM potassium ferrocyanide, 5 mM potassium ferricyanide, 150 mM NaCl, 2 mM MgCl₂) and incubated at $37\text{ }^{\circ}\text{C}$ for 12–16 h.

2.5. Dynamic Monitoring of Cell Adhesion by iCELLigence™

The RTCA iCELLigence™ system (ACEA Bioscience, Inc., Santa Clara, CA, USA) records impedance in real-time and converts into cell index (CI) [22]. This can quickly analyze cell adhesion ability and cell size during cell proliferation. The LS-BHK-21, BHK-21-parental and HS-BHK-21 cells were loaded into E-Plate L8 (ACEA Biosciences, Inc., Santa Clara, CA, USA) at 2×10^4 cells/well and the CI was recorded at 5-min intervals for the first 12 hr and then at 15-min intervals until the end of the measurement period. This is convenient to monitor the cell adhesion ability and cell events during the culture period, which can clearly distinguish different subclonal cells. The two subclonal cells were analyzed by iCELLigence equipment and compared with the BHK-21 parental cells.

2.6. Relative Cell Viability Calculation

Two BHK-21 subclones with significantly high and low SA- β -gal staining levels were isolated and named HS-BHK-21 (for high-staining) and LS-BHK-21 (for low-staining). The BHK-21-parental and two subclones, HS-BHK-21 and LS-BHK-21 cells, were seeded in 6-well plates 1 day before experiment. At about 60% confluence, the subclones were infected with BEFV (MOI = 0.01) and the mock group was incubated with MEM media only. After 48 hr, all experimental groups were trypsinized and counted by hemocytometer under the microscope. Relative cells viability was described by the following equation: relative cells viability = (virus infected group/mock group) \times 100%.

2.7. Camptothecin (CPT)-Induced Cell Senescence-Like Response

Cells (2×10^5 /per well) were seeded in 6 well plates and cultured overnight. CPT were diluted in culture media (250 nM final concentration) and added into the cells. After a 24 hr treatment, cells were infected BEFV at an MOI of 0.01. After the indicated incubation time, the cell images, virus supernatant, cell lysate or total mRNA were harvested. The virus supernatants were tittered by TCID₅₀.

2.8. Western Blot Analysis for BEFV N Protein

The cells were lysed in the RIPA solution (Tools, Co. Ltd., Taipei, Taiwan). The protein samples were determined by BCA protein assay (Pierce, Rockford, IL, USA), resolved by SDS-PAGE (20 µg/well), and transferred onto a polyvinylidene difluoride membrane (PerkinElmer, Massachusetts, USA). After blocking in Hyblock 1 min Blocking Buffer (Goalbio, Taipei, Taiwan) for 1 min at room temperature and by PBST washing (PBS containing 0.05% Tween-20), the membrane was blotted with mouse anti-BEFV N protein antiserum (1:1000) [23]. After PBST wash, the membrane was incubated with goat anti-mouse IgG-HRP (1:5000) antibody. The signal was developed by the ECL plus Western Blot Detection Reagents (GE Healthcare, Waukesha, WI, USA).

2.9. qRT-PCR for Senescence Related Gene Expression

Cellular total RNA was harvested and isolated by QIAzol Lysis Reagent (Qiagen, Hilden, Germany). Two micrograms of total RNA were reverse-transcribed with SensiFAST™ cDNA Synthesis Kit (Bioline, Memphis, TN, USA). The amounts of p16, p21, IL-6 and β-actin cDNA were determined by QuantiFast SYBR Green PCR Master Mix (Qiagen, Hilden, Germany) at the conditions: 95 °C for 3 min and 40 cycles of 95 °C for 15 s, 60 °C for 30 s and 72 °C for 15 s. Primers for each target gene were: p16-F: 5'-TCTTGAAACTCTGGCGATA-3', p16-R: 5'-GAAGTTACGCCTGCCG-3', p21-F: 5'-AGTGTGCCGCCGTCTCT-3', p21-R: 5'-ACACCAGAGT GCAGGACAGC-3', IL-6-F: 5'-GTCGGAGGTTTGGTTACATA-3', IL-6-R: 5'-ATCTGGACCCTTTACCTCTT-3' and β-actin-F: 5'-CCAAGCCAACCGTGA AAAG-3', β-actin-R: 5'-TGGCCATCTCTTGCTCGAAGTC-3'. The threshold cycle (CT) value of each target gene was normalized to the β-actin gene, and the mock control group using the $2^{-\Delta\Delta CT}$ method [24].

2.10. Statistical Analysis

Experimental data are expressed as mean ± sd. Statistical analysis of variance between groups was performed by the R Statistics software (4.0.3) with agricolae package. Additional statistical enrichment analyses of GSEA results were performed using the Hypergeometric test to measure the significance. Significant difference was set at 0.05 ($p < 0.05$) for all statistical tests.

3. Results

3.1. BEFV-Infected BHK-21 Cells Showed Morphological Changes and Upregulated Senescence-Related Gene Sets

To study BHK-21 cells' response to virus infection, experimental infection with BEFV was performed. Infected BHK-21 cells show an obvious cytopathic effect (CPE) and cell death. However, some cells survived and became persistently infected, showing enlarged and flattened morphology with apparently more vacuoles inside (Figure 1 in BEFV 48 hr). These cells can be passaged (Figure 1 in persistent BEFV-infected BHK-21 (p3)) and variable levels of BEFV can be detected (Table 1). To investigate potential gene expression changes within the cells after infection, Gene Set Enrichment Analysis (GSEA) was performed for BHK-21 cells under three conditions: (1) BEFV 24 h.p.i., (2) BEFV 48 h.p.i., and (3) BEFV persistent, when compared with uninfected BHK-21-parental cells. The results showed that senescence-related gene subsets were enriched for all three experimental groups (5, 15 and 9 aging/senescence gene subsets for group 1, 2 and 3, respectively), demonstrating that aging/senescence gene subsets were upregulated in response to virus infection. The regulation of virus infection in cells showed a discontinuous process. Firstly, immune/adhesion-related gene subsets were regulated to respond to virus infection after 24 hr (Figure 2, in BEFV 24 h.p.i.). At 48 h.p.i. and in BEFV-persistent cells, aging/senescence-related gene subsets were significantly upregulated (Figure 2, in BEFV 48 h.p.i. and BEFV persistent). These results suggest that aging/senescence gene subset upregulation is a potential mechanism for BHK-21 cells to counter BEFV infection.

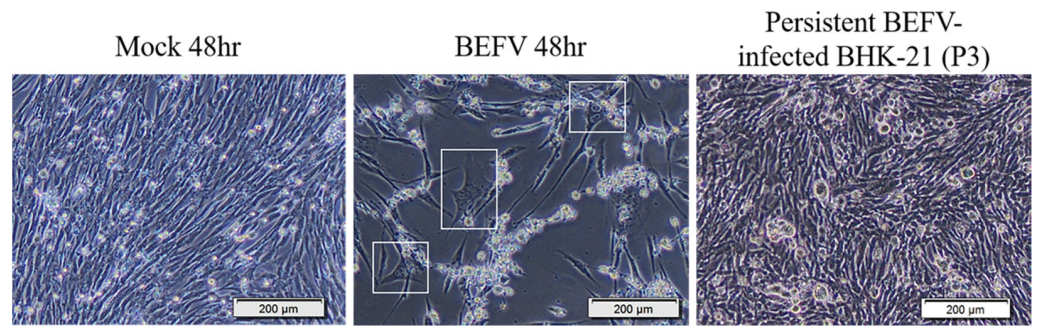


Figure 1. The BHK-21 Cell morphology changes in BEFV infection. Mock 48 hr: The BHK-21 cells were mock infected for 48 hr. BEFV 48 hr: The BHK-21 cells were infected with BEFV for 48 hr. Persistent BEFV infected BHK-21 cells (p3): The BEFV-infected BHK-21 cells survived and maintained their culture (passed 3 times). The cells were imaged with 400× microscope, and the scale bar showed 200 µm.

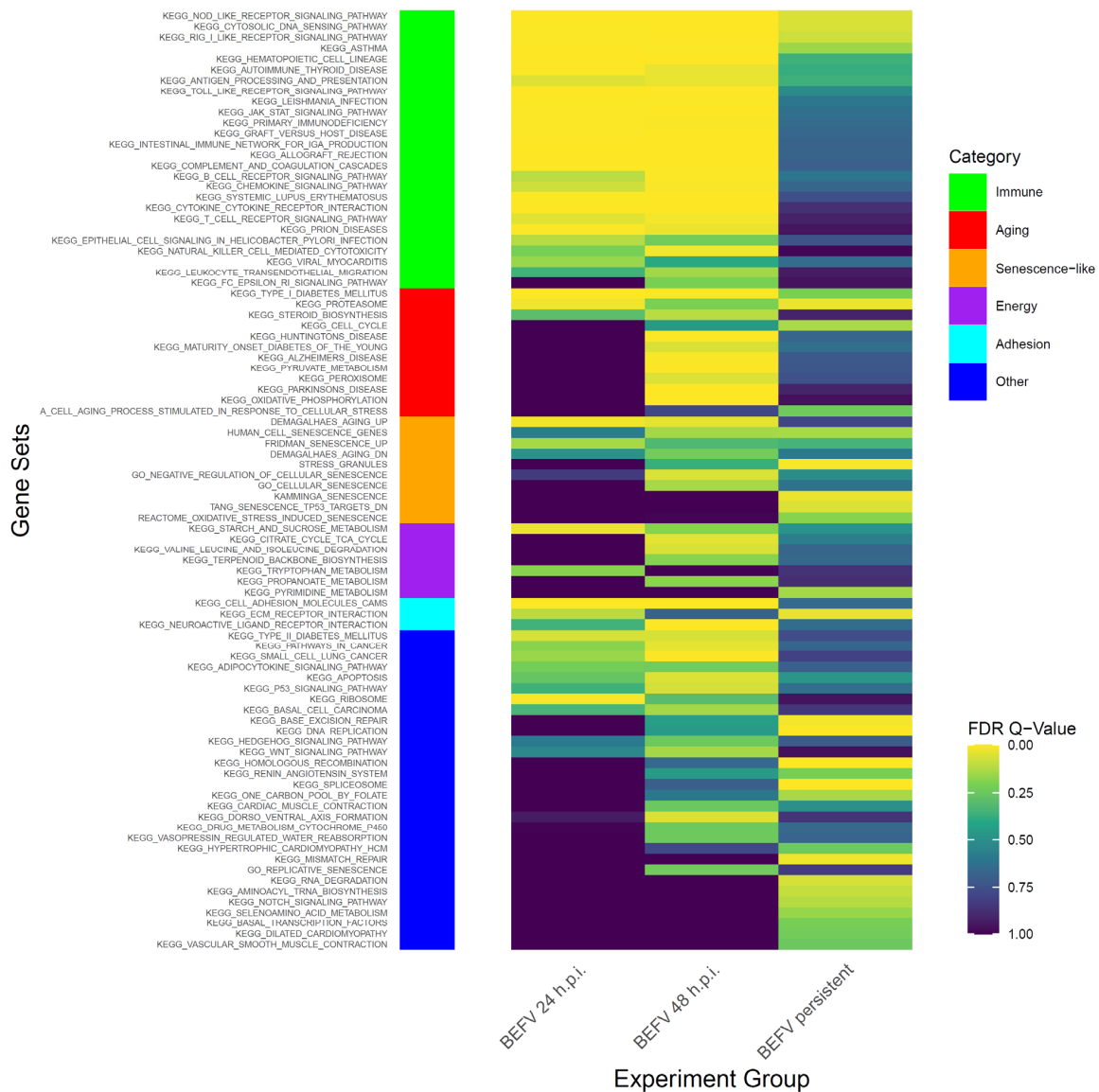


Figure 2. The GSEA results show enriched gene subsets in KEGG pathway with senescence related gene subsets. The data demonstrate FDR value (<0.25) in KEGG pathway at least significance in one experiment group. Side bar in left shows categories of gene subsets.

Table 1. Virus titer of the persistent BEFV-infected BHK-21 cells.

Persistent BEFV-Infected BHK-21	TCID ₅₀ *
Passage 7 cells	10 ^{1.8}
Passage 8 cells	10 ^{5.2}
Passage 9 cells	10 ^{4.4}
Passage 10 cells	10 ^{2.1}

* The virus titer were determined by qRT-PCR and compare to the standard virus.

3.2. BHK-21 Subclones in Senescence-Like State Are More Resistant to BEFV Infection

In a slightly different approach, we demonstrated that there are subclones of BHK-21 that show high extent of senescence-like state and are found to be more resistant to BEFV infection. A total of 36 BHK-21 subclones were established from the parental cell line using the limiting dilution method. The subclones were then stained with a general senescence-like cellular response marker, SA-β-gal, to determine the extent of senescence-like state (Supplementary Figure S1). Two BHK-21 subclones with significantly high and low SA-β-gal staining levels were picked and named HS-BHK-21 (for high-staining) and LS-BHK-21 (for low-staining) (Figure 3A). The average of SA-β-gal staining positive ratios in HS-BHK-21, LS-BHK-21 cells and parental BHK-21 cells are 33%, <0.1% and 0.9%, respectively (Supplementary Figure S2). Cell growth analysis in the iCELLigence system showed that HS-BHK-21 has a higher adhesion ability and a larger cell size while LS-BHK-21 resembles the parental BHK-21. The HS-BHK-21 cells showed a significantly higher cell index than others in the first 4 h culture when they all start with the same cell number (Figure 3B). Upon BEFV infection, HS-BHK-21 showed significantly lower virus titer (85%) when compared to the parental and LS-BHK-21 (Figure 3C), linking higher senescence-like state with resistance to virus infection.

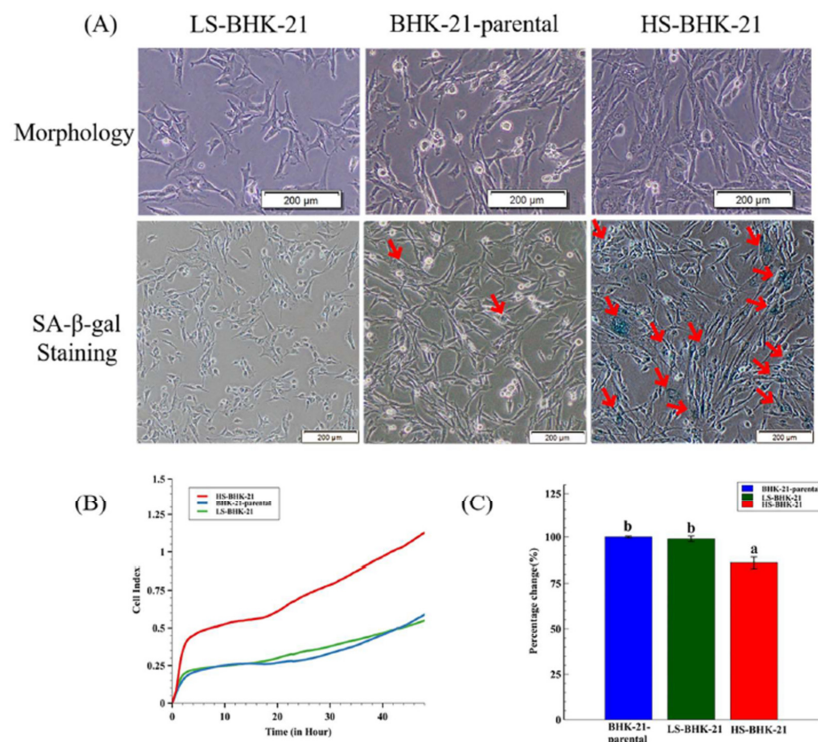


Figure 3. The different SA-β-gal staining property and the virus production of subclonal BHK-21 cells. (A) Cell morphology and the SA-β-gal staining results for LS-BHK-21, parental and the HS-BHK-21 cells. The cells were imaged with 400× microscope, and the scale bar shows 200 μm. (B) The adhesion properties and cell events of the parental and subclonal cells are showed as cell index curve which is measured by RTCA iCELLigence™. (C) The particular BEFV titer (48 h.p.i.) cultured by the parental and subclonal cells were compared to the BHK-21-parental group and showed as percentage. Fold change means with different letters are significantly different (Tukey's HSD, $p < 0.05$).

To mimic virus passage during industrial scale virus production, we further investigated how virus titer may change with serial passage of BEFV in the BHK-21 subclones (Figure 4A). Results showed that, for three passages, BEFV titers remained low in HS-BHK-21 when compared to LS-BHK-21 and parental BHK-21 (Figure 4B). This indicates that culturing BEFV in HS-BHK-21 cells may further inhibit virus replication during serial passage. The survival rate of the subclones after each round of virus infection was also tracked (Figure 4C). The three cell populations showed significantly different cell viability after BEFV infection (HS-BHK-21 > BHK-21-parental > LS-BHK-21). HS-BHK-21 showed remarkable resistance to BEFV induced CPE in passage 3. The time-lapse CPE image records in three different senescence states also confirmed the results (<https://youtu.be/bVz9VxudRLo>, accessed on 3 June 2021). These results indicated that culturing BEFV in HS-BHK-21 cells may further inhibit the virus replication in the following virus passages. A senescence-like cellular function change that may enhance anti-viral response in BHK-21 cells was discovered.

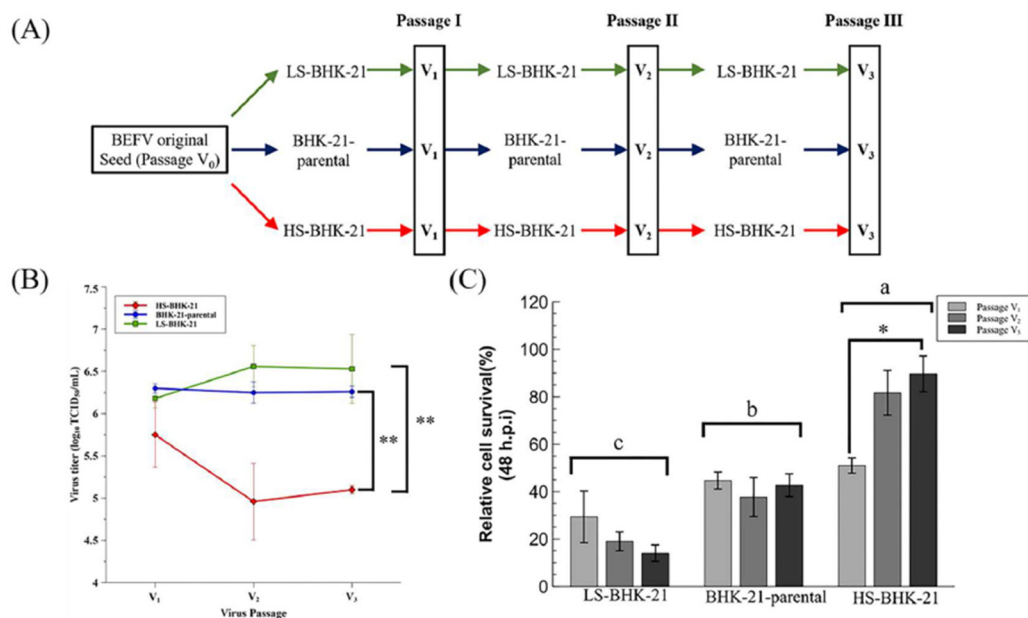


Figure 4. The virus production ability of the parental and subclonal cells in serial virus passages. **(A)** The three serial passages experiment design was showed. **(B)** The virus supernatant of the three continuous serial passages in three different cells population were harvested at 48 h.p.i., and determined by TCID₅₀ assay. **(C)** The relative cell survival percentage of the parental and subclonal cells were determined at 48 h.p.i. by directly trypsinized cell counting, and the percentage was compared to the mock infection, respectively. Three independent repeats were performed, and were analyzed by one-way ANOVA. Means with different letters are significantly different (Tukey's HSD, $p < 0.05$). * $p < 0.05$, ** $p < 0.01$ compared to indicated group.

3.3. BHK-21 in Drug-Induced Senescence-Like State Is More Resistant to BEFV Infection

Since a senescence-like state is drug-inducible, we investigated whether BHK-21 in this drug-induced senescence-like state is more resistant to BEFV infection. In a previous study, the small molecule, camptothecin (CPT), showed high efficiency when inducing BHK-21 cells into a senescence state [25]. Here, this small molecular was employed to induce senescence in BHK-21 cells in three senescence state. Upon CPT treatment for 24 hr, all cells showed an enlarged size and positive SA- β -gal staining (Figure 5A upper panel), giving signs of a senescence-like state. When the treated cells were infected with BEFV, cytopathic effect was significantly inhibited compared to the untreated control (Figure 5A lower panel). A 100-fold decrease in virus titer was observed when compared to the untreated cells (Figure 5B). Additionally, in the CPT-treated cells, BEFV viral protein N was detected long after infection at 48 h.p.i., versus 24 h.p.i., for the untreated cells (Figure 6A).

These results illustrated that BHK-21 in CPT-induced senescence-like state is much less permissible to virus infection. At the gene expression level, further analysis was performed with common senescence-like markers p16, p21, and IL-6 (Figure 6B). Gene expression for p16 was significantly higher in the CPT-pretreated and BEFV 48 h.p.i. groups. For the p12 gene, expression significantly increased in all CPT-treated groups; notably, the expression was even higher for the BEFV 48 h.p.i. group. IL-6 gene expression was significantly higher only after virus infection. Interestingly, p16 and IL-6 gene overexpression was significant in the CPT which was pretreated only after BEFV infection for 48 hr. Overall, these results suggest that a senescence-like state was induced by CPT in the BHK-21 cells, and upon virus infection, further gene expression change may be observed.

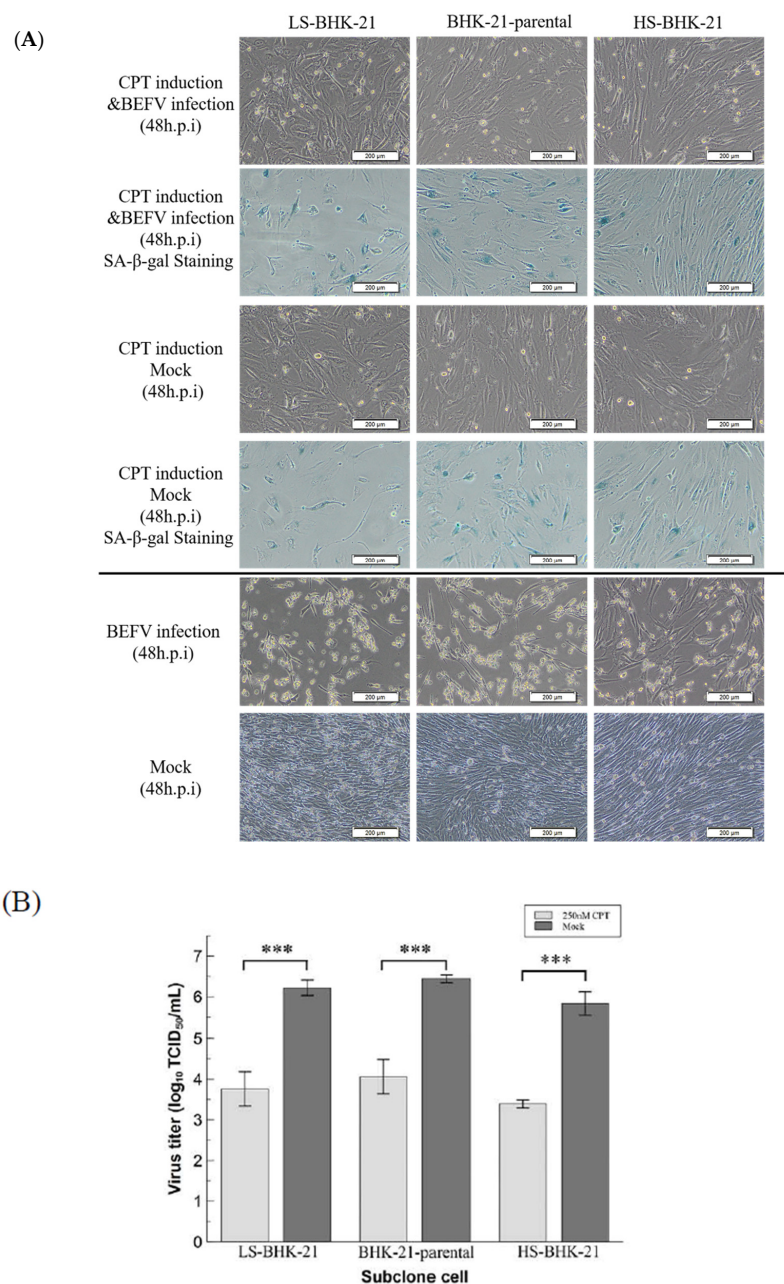


Figure 5. CPT induced senescence-like cell response inhibited virus replication in BHK-21 parental and subclonal cells. (A) The parental and subclonal cells were pretreated with or without CPT (250 nM) for 24 hr, and then infected by BEFV. The senescence-like cell response was determined by SA-β-gal staining and imaged by 400× microscope, and the scale bar shows 200 μm. (B) The virus titer in the supernatant from CPT pretreatment assay ($n = 3$) were analyzed by TCID₅₀ and analyzed by *t*-test. *** $p < 0.001$.

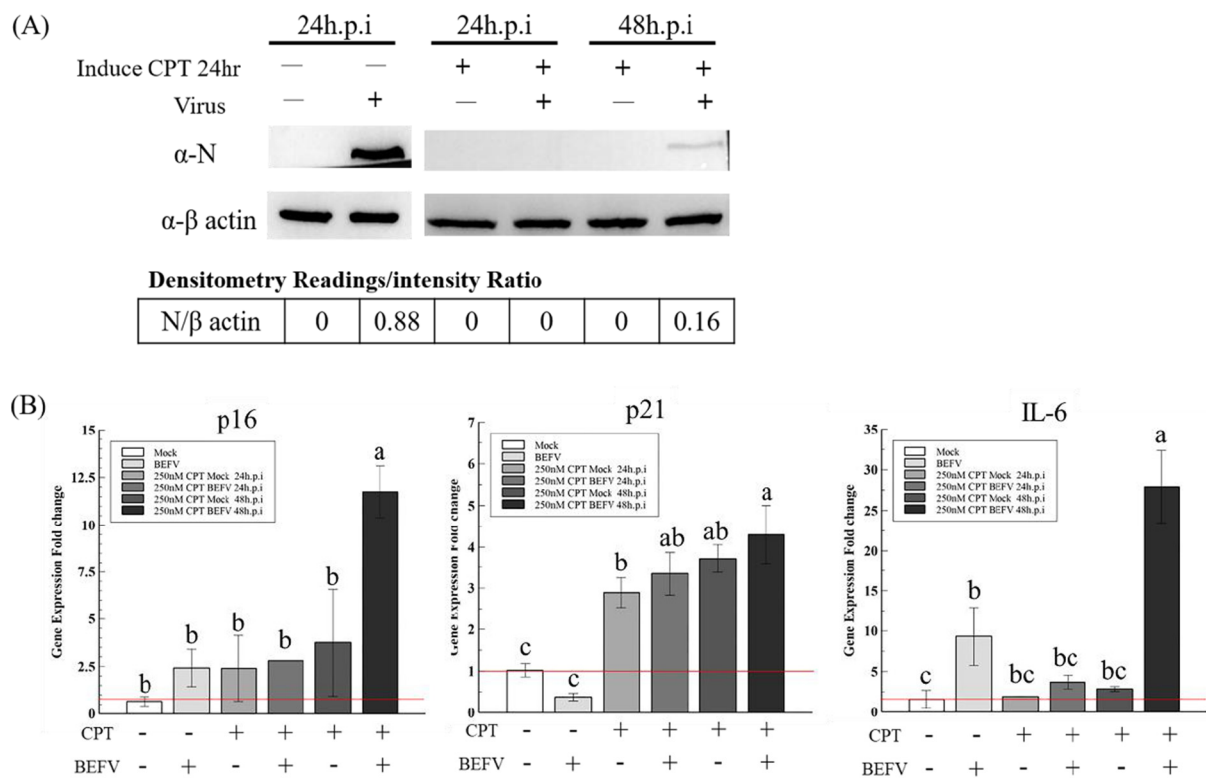


Figure 6. The CPT induced senescence-like response markers, P16, P21 and IL-6, in BHK-21-parental cells with or without BEFV infection. (A) The BHK-21-parental cells were pretreated by CPT for 24 h and followed the BEFV infection for 24 and 48 hr, as indicated. The virus was detected by Western blotting with the mouse anti-viral protein N antiserum. (B) The cell p16, p21 and IL-6 gene expression in (A) were analyzed by the qRT-PCR respectively and showed as gene expression fold change compared to mock (red line indicate 1-fold). Means with different letters are significantly different (Tukey's HSD, $p < 0.05$).

4. Discussion

In this study, we provided a survey of functional gene sets that are affected in BHK-21 upon BEFV infection. Gene set results and cell characteristics together suggested a senescence-like cellular response to viral infection. We further found that subclones of BHK-21 with high senescence marker staining are resistant to BEFV infection. Conversely, BHK-21 subclones with low senescence staining are permissible to virus replication, and therefore may be better suited for large-scale bioreactors.

The definition of senescence has been controversial and definitive characterization of the senescent state may be difficult. When first discovered, senescence was associated with DNA damage and telomere shortening. More recent studies found that senescence is a gradually progressing process [26,27]. Senescence-like characteristics may even reverse course before the cell goes into total functional arrest and cell death [28]. Furthermore, numerous genes are associated with cell senescence, for example, the p53, p21, p16, and IL-16 [12,29,30]. In our study, not all markers were examined and induced senescent state may or may not be true senescence, and therefore we used the qualifier 'senescence-like' cell response.

According to the SA- β -gal staining protocol, a cell would be stained positive at pH6.0 when it overexpresses and accumulates endogenous lysosomal beta-galactosidase [31]. As described in the previous section, the senescence-like characteristics may not be fixed and may even be reversed. This also explains why the HS-BHK-21 cells did not all show positive SA- β -gal staining at the same time (Figures 3A and 5A). This staining method can only help us distinguish the cell population with different senescence-like characteristics. However, the BEFV still could successfully penetrate the cells and produce viral nucleoprotein in both SA- β -gal staining positive or negative cells (Supplementary Figure S3). This indicates

that the SA-B-Gal staining positive cells may not directly inhibit the BEFV attachment and penetration. The molecular mechanism of the HS-BHK-21 cells interfering with virus production still needs further research.

During our serial passaging of BEFV in different BHK-21 subclones, we observed a dramatic decrease in virus titer for the HS-BHK-21 subclone, which exhibits high senescence staining. Furthermore, both subclonal cells (HS-BHK-21 and LS-BHK-21) can keep their own SA- β -gal staining characteristics for more than 10 passages in the general culture condition (data not shown). We suspect that the senescence-associated secretory phenotype (SASP) may be at play. Senescent cells are known to exhibit SASP, which includes the secretion of cytokine, chemokine, extracellular matrix protease, growth factor, and other signaling molecules that can induce senescence in neighboring cells [32]. Baz-Martínez M. and colleagues reported that drug-induced senescent A549 cells showed SASP and made daughter cells resistant to vesicular stomatitis virus infection [33]. In our study, it is possible that HS-BHK-21 secreted SASP signals into the virus supernatant and resulted in the inhibition of virus replication in the following culture passages. The SASP may be the cause of virus titer instability in cell culture systems, especially for high-density bioreactor with a large cell amplifying ratio. However, the type and composition of this SASP in the HS-BHK-21 cells need further study in the future. There are two ways to solve this unstable virus titer problem: the first is the employment of low senescence cells such as the LS-BHK-21 subclone; the second is to adjust the culture media with anti-oxidation or anti-aging components.

5. Conclusions

We described a senescence-like cell response in BHK-21 after BEFV infection. BHK-21 subclones showing high senescence staining could inhibit BEFV replication while low senescence-staining subclones are permissive to virus replication. The subclones could have utility in virus production for vaccine purposes and can be used for study to develop non-specific anti-viral molecules.

Supplementary Materials: The following are available online at <https://www.mdpi.com/article/10.3390/vaccines9060601/s1>, Table S1: External senescence-related gene subsets added in the analysis title, Figure S1: Cell morphology and SA- β -gal stained images of 36 BHK-21 subclones, Figure S2: The SA- β -gal staining positive cell ratio in parental and subclonal BHK-21 cells, Figure S3: The BEFV can infect all three BHK-21 clonal cells.

Author Contributions: H.-Y.W. designed the study. Y.-J.Z. performed the virus infection assay, protein analysis and gene expression. M.-K.H. analyzed the total mRNA expression for the cell functional analysis. C.-A.T. isolated the subclonal cells. C.-Y.C. provided the virus and helped to interpret the data. H.-C.W. help to analyze and interpret the data. Y.-J.Z. and H.-Y.W. wrote this paper. All authors have read and agreed to the published version of the manuscript.

Funding: This study was supported by a grant from the Ministry of Science and Technology, Taiwan, R.O.C. (MOST 107-2313-B-020-003 and MOST 109-2313-B-020-005). The funding agency played no role in study design, data analysis, or manuscript writing.

Institutional Review Board Statement: Not applicable.

Informed Consent Statement: Not applicable.

Data Availability Statement: The datasets used and analyzed during the current study are available from the corresponding author on reasonable request.

Acknowledgments: We are very thankful to Li-Ting Cheng in National Pingtung University of Science and Technology for the language editing and the paper reviewing.

Conflicts of Interest: The authors declare that they have no competing interest.

References

1. Emeny, J.M.; Morgan, M.J. Regulation of the interferon system: Evidence that vero cells have a genetic defect in interferon production. *J. Gen. Virol.* **1979**, *43*, 247–252. [[CrossRef](#)]
2. Nagai, Y.; Ito, Y.; Hamaguchi, M.; Yoshida, T.; Matsumoto, T. Relation of interferon production to the limited replication of Newcastle disease virus in L cells. *J. Gen. Virol.* **1981**, *55*, 109–116. Available online: <https://pubmed.ncbi.nlm.nih.gov/6170723/> (accessed on 9 December 2020). [[CrossRef](#)]
3. Genzel, Y. Designing cell lines for viral vaccine production: Where do we stand? *Biotechnol. J.* **2015**, *10*, 728–740. [[CrossRef](#)]
4. Hsieh, Y.-C.; Wang, S.-Y.; Lee, Y.-F.; Chen, S.-H.; Mak, P.O.T.; Chu, C.-Y. DNA sequence analysis of glycoprotein G gene of bovine ephemeral fever virus and development of a double oil emulsion vaccine against bovine ephemeral fever. *J. Vet. Med. Sci.* **2006**, *68*, 543–548. [[CrossRef](#)]
5. Chung, Y.C.; Shen, H.Y.; Cheng, L.T.; Liu, S.S.; Chu, C.Y. Effectiveness of a BHV-1/BEFV bivalent vaccine against bovine herpesvirus type 1 infection in cattle. *Res. Vet. Sci.* **2016**, *109*, 161–165. [[CrossRef](#)] [[PubMed](#)]
6. Zheng, F.; Qiu, C. Phylogenetic relationships of the glycoprotein gene of bovine ephemeral fever virus isolated from mainland China, Taiwan, Japan, Turkey, Israel and Australia. *Virol. J.* **2012**, *9*, 268. [[CrossRef](#)] [[PubMed](#)]
7. Walker, P.J.; Klement, E. Epidemiology and control of bovine ephemeral fever. *Vet. Res.* **2015**, *46*, 124. [[CrossRef](#)] [[PubMed](#)]
8. Ting, L.J.; Lee, M.S.; Lin, Y.L.; Cheng, M.C.; Lee, F. Invasion of exotic bovine ephemeral fever virus into Taiwan in 2013–2014. *Vet. Microbiol.* **2016**, *182*, 15–17. [[CrossRef](#)] [[PubMed](#)]
9. Aziz-Boaron, O.; Gleser, D.; Yadin, H.; Gelman, B.; Kedmi, M.; Galon, N.; Klement, E. The protective effectiveness of an inactivated bovine ephemeral fever virus vaccine. *Vet. Microbiol.* **2014**, *173*, 1–8. [[CrossRef](#)] [[PubMed](#)]
10. Han, L.; Xin, X.; Wang, H.; Li, J.; Hao, Y.; Wang, M.; Zheng, C.; Shen, C. Cellular response to persistent foot-and-mouth disease virus infection is linked to specific types of alterations in the host cell transcriptome. *Sci. Rep.* **2018**, *8*, 1–13. [[CrossRef](#)]
11. Wild, T.F.; Bijlenga, G. A rabies virus persistent infection in BHK21 cells. *J. Gen. Virol.* **1981**, *57*, 169–177. [[CrossRef](#)]
12. Hernandez-Segura, A.; Nehme, J.; Demaria, M. Hallmarks of Cellular Senescence. *Trends Cell Biol.* **2018**, *28*, 436–453. [[CrossRef](#)] [[PubMed](#)]
13. Kowalski, P.; Dihel, N.; Garcia, M. India. In *Emerging Economies*; OECD: Paris, France, 2008; Chapter 8, pp. 283–331.
14. MuenchL, J.R.H. A simple method of estimating fifty per cent endpoints. *Hygiene* **1938**, *27*, 493–497.
15. Dobin, A.; Gingeras, T.R.; Spring, C.; Flores, R.; Sampson, J.; Knight, R. Mapping RNA-seq with STAR. *Curr. Protoc. Bioinform.* **2016**, *51*, 586–597.
16. Dobin, A.; Davis, C.A.; Schlesinger, F.; Drenkow, J.; Zaleski, C.; Jha, S.; Batut, P.; Chaisson, M.; Gingeras, T.R. STAR: Ultrafast universal RNA-seq aligner. *Bioinformatics* **2013**, *29*, 15–21. [[CrossRef](#)] [[PubMed](#)]
17. Trapnell, C.; Williams, B.A.; Pertea, G.; Mortazavi, A.; Kwan, G.; Van Baren, M.J.; Salzberg, S.L.; Wold, B.J.; Pachter, L. Transcript assembly and quantification by RNA-Seq reveals unannotated transcripts and isoform switching during cell differentiation. *Nat. Biotechnol.* **2010**, *28*, 511–515. [[CrossRef](#)] [[PubMed](#)]
18. Subramanian, A.; Tamayo, P.; Mootha, V.K.; Mukherjee, S.; Ebert, B.L.; Gillette, M.A.; Paulovich, A.; Pomeroy, S.L.; Golub, T.R.; Lander, E.S.; et al. Gene set enrichment analysis: A knowledge-based approach for interpreting genome-wide expression profiles. *Proc. Natl. Acad. Sci. USA* **2005**, *102*, 15545–15550. [[CrossRef](#)] [[PubMed](#)]
19. Mootha, V.K.; Lindgren, C.M.; Eriksson, K.F.; Subramanian, A.; Sihag, S.; Lehar, J.; Puigserver, P.; Carlsson, E.; Ridderstrale, M.; Laurila, E.; et al. PGC-1 α -Responsive Genes Involved in Oxidative Phosphorylation Are Coordinately Downregulated in Human Diabetes. *Nat. Genet.* **2003**, *34*, 267–273. [[CrossRef](#)]
20. Kuilman, T.; Michaloglou, C.; Mooi, W.J.; Peeper, D.S. The essence of senescence. *Genes Dev.* **2010**, *24*, 2463–2479. [[CrossRef](#)]
21. Dimri, G.P.; Lee, X.; Basile, G.; Acosta, M.; Scott, G.; Roskelley, C.; Medrano, E.E.; Linskens, M.; Rubelj, I.; Pereira-Smith, O. A biomarker that identifies senescent human cells in culture and in aging skin in vivo. *Proc. Natl. Acad. Sci. USA* **1995**, *92*, 9363–9367. [[CrossRef](#)]
22. Hamidi, H.; Lilja, J.; Ivaska, J. Using xCELLigence RTCA Instrument to Measure Cell Adhesion. *Bio-Protocol* **2017**, *7*, e2646. [[CrossRef](#)]
23. Cheng, L.T.; Zeng, Y.J.; Chu, C.Y.; Wang, H.Y. Development of a quick dot blot assay for the titering of bovine ephemeral fever virus. *BMC Vet. Res.* **2019**, *15*, 313. [[CrossRef](#)]
24. Livak, K.J.; Schmittgen, T.D. Analysis of relative gene expression data using real-time quantitative PCR and the 2- $\Delta\Delta$ CT method. *Methods* **2001**, *25*, 402–408. [[CrossRef](#)]
25. Cheng, H.L.; Chang, S.M.; Cheng, Y.W.; Liu, H.J.; Chen, Y.C. Characterization of the activities of p21Cip1/Waf1 promoter-driven reporter systems during camptothecin-induced senescence-like state of BHK-21 cells. *Mol. Cell. Biochem.* **2006**, *291*, 29–38. [[CrossRef](#)] [[PubMed](#)]
26. Johmura, Y.; Nakanishi, M. Multiple facets of p53 in senescence induction and maintenance. *Cancer Sci.* **2016**, *107*, 1550–1555. [[CrossRef](#)]
27. Herranz, N.; Gil, J. Mechanisms and functions of cellular senescence. *J. Clin. Investig.* **2018**, *128*, 1238–1246. [[CrossRef](#)]
28. Wengerodt, D.; Schmeer, C.; Witte, O.W.; Kretz, A. Amitosenescence and Pseudomitosenescence: Putative New Players in the Aging Process. *Cells* **2019**, *8*, 1546. [[CrossRef](#)]
29. Yusu, F.; Terzi, M.; Izmirlı, M.; Gogebakan, B. The cell fate: Senescence or quiescence. *Mol. Biol. Rep.* **2016**, *43*, 1213–1220.

30. Ovadya, Y.; Krizhanovsky, V.; Ovadya, Y.; Krizhanovsky, V. Strategies targeting cellular senescence Find the latest version: Strategies targeting cellular senescence. *J. Clin. Investig.* **2018**, *128*, 1247–1254. [[CrossRef](#)]
31. Lee, B.Y.; Han, J.A.; Im, J.S.; Morrone, A.; Johung, K.; Goodwin, E.C.; Kleijer, W.J.; DiMaio, D.; Hwang, E.S. Senescence-associated β -galactosidase is lysosomal β -galactosidase. *Aging Cell* **2006**, *5*, 187–195. [[CrossRef](#)]
32. Hoare, M.; Das, T.; Alexander, G. Ageing, telomeres, senescence, and liver injury. *J. Hepatol.* **2010**, *53*, 950–961. [[CrossRef](#)]
33. Baz-Martínez, M.; Da Silva-Álvarez, S.; Rodríguez, E.; Guerra, J.; El Motiam, A.; Vidal, A.; García-Caballero, T.; González-Barcia, M.; Sánchez, L.; Muñoz-Fontela, C.; et al. Cell senescence is an antiviral defense mechanism. *Sci. Rep.* **2016**, *6*, 37007. [[CrossRef](#)] [[PubMed](#)]